



Comparative development and ocular histology between epigeal and subterranean salamanders (*Eurycea*) from central Texas

Ruben U. Tovar^{1,2} Valentin Cantu^{3,4} Brian Fremaux¹ Pedro Gonzalez Jr¹
Amanda Spikes¹ Dana M. García¹

¹ Department of Biology, Texas State University, San Marcos, TX, United States of America

² Department of Integrative Biology, University of Texas at Austin, Austin, TX, United States of America

³ San Marcos Aquatic Resources Center, U.S. Fish and Wildlife Service, San Marcos, TX, United States of America

⁴ Uvalde National Fish Hatchery, U.S. Fish and Wildlife Service, Uvalde, TX, United States of America

ABSTRACT

The salamander clade *Eurycea* from the karst regions of central Texas provides an ideal platform for comparing divergent nervous and sensory systems since some species exhibit extreme phenotypes thought to be associated with inhabiting a subterranean environment, including highly reduced eyes, while others retain an ancestral ocular phenotype appropriate for life above ground. We describe ocular morphology, comparing three salamander species representing two phenotypes—the surface-dwelling Barton Springs salamander (*E. sosorum*) and San Marcos salamander (*E. nana*) and the obligate subterranean Texas blind salamander (*E. rathbuni*) - in terms of structure and size of their eyes. Eyes were examined using confocal microscopy and measurements were made using ImageJ. Statistical analysis of data was carried out using R. We also provide a developmental series and track eye development and immunolocalization of Pax6 in *E. sosorum* and *E. rathbuni*. Adult histology of the surface-dwelling San Marcos salamander (*E. nana*) shows similarities to *E. sosorum*. The eyes of adults of the epigeal species *E. nana* and *E. sosorum* appear fully developed with all the histological features of a fully functional eye. In contrast, the eyes of *E. rathbuni* adults have fewer layers, lack lenses and other features associated with vision as has been reported previously. However, in early developmental stages eye morphology did not differ significantly between *E. rathbuni* and *E. sosorum*. Parallel development is observed between the two phenotypes in terms of morphology; however, Pax6 labeling seems to decrease in the latter stages of development in *E. rathbuni*. We test for immunolabeling of the visual pigment proteins opsin and rhodopsin and observe immunolocalization around photoreceptor disks in *E. nana* and *E. sosorum*, but not in the subterranean *E. rathbuni*. Our results from examining developing salamanders suggest a combination of underdevelopment and degeneration contribute to the reduced eyes of adult *E. rathbuni*.

Submitted 20 October 2018

Accepted 1 July 2021

Published 28 July 2021

Corresponding author

Ruben U. Tovar, rubenut@utexas.edu

Academic editor

Mason Posner

Additional Information and
Declarations can be found on
page 15

DOI 10.7717/peerj.11840

© Copyright
2021 Tovar et al.

Distributed under
Creative Commons CC-BY 4.0

OPEN ACCESS

Subjects Developmental Biology, Evolutionary Studies

Keywords Ocular development, Divergent evolution, Evolution and development, Subterranean salamander

INTRODUCTION

Subterranean environments exert strong selective pressures on organisms that occupy them. Additionally, relaxed selection can be equally pervasive when an organism invades a novel subterranean niche. Both scenarios seem to apply to vertebrates that occupy subterranean environments ([Rétaux & Casane, 2013](#)), resulting in their convergent evolution. Arguably, a quintessential phenotype of subterranean organisms is the reduction of the eye, which may reflect a combination of relaxed selection, directional selection, and genetic drift ([Rétaux & Casane, 2013](#)). Eye reduction can be observed in organisms that occupy both terrestrial and aquatic subterranean environments. Terrestrial organisms that occupy dim light environments such as caves (trogllobites) and fossorial niches share in a range of eye reduction, as is the case with cave beetles and some fossorial mammals, such as moles ([Rétaux & Casane, 2013](#)).

Obligate aquatic subterranean fauna are referred to as stygobites ([Goricki, Niemiller & Fenolio, 2012](#)). Similar to trogllobites, stygobitic morphology includes drastically reduced eyes and pale skin; however, aquatic environments differ from terrestrial environments (e.g., conductivity) and could impose different selective pressures ([Rohner et al., 2013](#)). Stygobitic vertebrates broadly fall into two major lineages, teleost and Caudates. Within Caudata, the genus *Eurycea* and *Proteus* show several occurrences of subterranean invasions. Two phenotypes have been recognized within the central European *P. anguinus* populations (*P. anguinus anguinus* and *P. anguinus parkelj*), showing differences in pigmentation and eye development with the former lacking pigmentation and eyes, and the latter being fully pigmented and exhibiting relatively more eye structure ([Durand, 1976](#)). Stygobitic morphology is exemplified in the genus *Eurycea* by the Texas blind salamander (*E. rathbuni*) with its reduced pigment and eye structure ([Mitchell & Reddell, 1965](#)). In contrast, the San Marcos salamander (*E. nana*) and Barton Springs salamander (*E. sosorum*) are surface species and have pigmented skin and seemingly well-developed eyes.

Ocular histology has been investigated in several families of salamanders ([Fite, 1976](#); [Linke, Roth & Rottluff, 1876](#); [Roth, 1987](#)), and differing degrees of ocular regression are documented in the subterranean species of the genera *Eurycea* ([Eigenmann, 1900](#); [Emerson, 1905](#)), *Eurycea spelaea* (formerly in the genus *Typhlotriton*; [Walls, 1942](#)), and *Proteus* ([Möller, 1951](#)). Among the cave dwelling species, the eye reduction observed in *E. rathbuni* is relatively extreme: the eye, completely surrounded by melanized tissue, lacks the distinct layers observed in organisms with vision. Eye reduction in *Proteus anguinus anguinus*, while not fully surrounded by pigment, nevertheless has a reduced photoreceptor population. In contrast, *E. spelaea* individuals experience partial eye reduction during and post metamorphosis ([Walls, 1942](#)). Although ocular histology has been examined in *E. rathbuni* ([Eigenmann, 1900](#)), no direct comparisons to surface relatives have been made, nor have the developmental processes leading to morphological divergence been examined. Such a comparison is of interest because it could shed light on the interaction between evolutionary and developmental processes that lead to the divergence of closely related species. Significantly, there have been a number of subterranean invasions by the central Texas *Eurycea*, and phylogenetic analyses show strong support for a close relationship

between the species with divergent ocular phenotypes ([Bendik et al., 2013](#); [Chippindale et al., 2000](#); [Wiens, Chippindale & Hillis, 2003](#); [Devitt et al., 2019](#)).

The *Astyanax mexicanus* system exemplifies closely related populations, an epigeal population and a styobitic (cavefish) population, with extremely divergent ocular phenotypes. Work by [Jeffery et al. \(2009\)](#) has shown that the loss of the eye in the cavefish can be partially rescued by transplanting the lens of an above-ground animal into a developing cavefish eye ([Krishnan & Rohner, 2017](#)). Furthermore, [Jeffery \(2005\)](#) has shown that loss of the eye in the cavefish is accompanied by upregulation of *sonic hedgehog* (*Shh*) and down-regulation of *paired homeobox protein-6* (*pax6*) preceding apoptosis of the lens tissue. In many species, Pax6 functions as a transcription factor and plays a role in the development of the anterior/posterior axis, the nervous system, and critically in eye development ([Wawersik & Maas, 2000](#)). Pax6's diminished expression leads to eye reduction in the Somalian teleost cavefish *Phreatichthys andruzzii*. Unlike *A. mexicanus*, *P. andruzzii* experiences retinal apoptosis driven by waves of apoptotic events during late retinal development ([Stemmer et al., 2015](#)), revealing yet another process by which eye reduction may be accomplished.

Herein we describe for the first time the ocular histology of two surface species of central Texas *Eurycea*, namely *E. nana* and *E. sosorum*. Additionally, we compare the ocular histology of the subterranean *E. rathbuni* to that of the surface species, augmenting the descriptive study provided by [Eigenmann \(1900\)](#). We use immunohistochemistry to test for presence of the visual pigments opsin and rhodopsin in the eyes of adult *E. rathbuni*, *E. sosorum* and *E. nana*. We compare the size of eyes in developing and adult salamanders and discuss whether the reduced eyes observed in *E. rathbuni* represent underdeveloped eyes or regressed eyes. Finally, we present the first developmental series for *E. sosorum* and *E. rathbuni*, and use immunohistochemistry to compare expression of Pax6, which has been shown to be divergent in surface and cave populations of Mexican tetra (*A. mexicanus*; [Jeffery, 2009](#)) and Somalian cavefish (*P. andruzzii*; [Stemmer et al., 2015](#)). Given the importance of Pax6 during eye development in amphibians ([Chow et al., 1999](#)), we hypothesize that downregulation of Pax6 may be important in the development of stygomorphy in salamanders. Parallels in Pax6 expression between salamanders and fishes are discussed.

MATERIALS & METHODS

Specimens

The San Marcos Aquatic Resource Center (SMARC), Texas, United States Fish and Wildlife Service (USFWS) donated freshly dead adult specimens of Texas blind salamander (*Eurycea rathbuni*; $n = 3$), San Marcos salamander (*E. nana*; $n = 3$), and Barton Springs salamander (*E. sosorum*; $n = 3$) to Texas State University in San Marcos, Texas. The specimens' heads were removed and transported to Texas State University for further processing under scientific permit number SPR-0390-045. General measurements along with tissue samples were taken from the remaining body which was then preserved in 95% ethanol and catalogued at SMARC. Embryos of *E. rathbuni* and *E. sosorum* were obtained from

captive populations at SMARC. Staging was determined by morphology ([Duellman & Trueb, 1986](#)), and embryos were imaged using a stereomicroscope equipped with a camera. All animal manipulations were approved by Texas State University Institutional Animal Care and Use Committee (IACUC protocol approval number 0222_0530_12).

Fixation and imaging

Techniques for fixation of heads and embryos followed [Neve et al. \(2012\)](#) as described below. Tissues were placed in 4% buffered paraformaldehyde for 24 h and washed three times for 10 minutes with phosphate buffered saline (PBS). Following fixation, tissues were placed in a 30% sucrose solution prepared in PBS for cryoprotection and stored at 4 °C for at least 24 h. Adult tissue sections were cut at 20 μm, mounted on a slide using 90% glycerol, and stored at −20 °C ([Saul, Koke & García, 2010](#)). At the conclusion of the study, sections were deposited at The University of Texas at Austin's Biodiversity Center. Images were acquired using an Olympus FV1000 equipped with differential interference contrast optics and a 10× objective.

Retinal and ocular measurements

Images of ocular sections were opened in ImageJ software ([Schneider, Rasband & Eliceiri, 2012](#)), and the measurement tool was calibrated to each image. One image from each individual representing the three species (*E. rathbuni*, $n = 3$; *E. nana*, $n = 3$; and *E. sosorum*, $n = 3$) was selected for measurement. For the epigeal species (*E. nana* and *E. sosorum*), the selection of the image was based on the presence of a lens in the section and six clearly distinguishable retinal layers: photoreceptor/retinal pigment epithelial layer, outer nuclear layer (ONL), outer plexiform layer (OPL), inner nuclear layer (INL), inner plexiform layer (IPL), and retinal ganglion cell layer (RGL). Measurements of retinal width were obtained from a region where the OPL appeared undistorted, signifying that the section in that region was not oblique. Three measurements were taken per individual with the transect being orthogonal to the OPL. Three measurements for each retinal layer were also obtained from each individual in the region of the transect. The means of the triplicate measurements were used to provide an estimate of thicknesses for that individual, and the three individuals provided an estimate of population means for their respective species ($n = 3$).

Thirty-four adult and three early developmental stage specimens for each species (*E. sosorum* and *E. rathbuni*) were obtained from SMARC and imaged using a Nikon D7000. Eye and head length measurements were obtained using ImageJ ([File S1](#)). Both eye and head measurements of each species were tested for normality. An analysis of variance (ANOVA) was conducted using eye measurements taken from adults and earlier developmental stages (standardized by head length) for each of the two species.

Immunohistochemistry and imaging

Immunohistochemistry using transverse sections of embryo eyes was accomplished by blocking with 3% bovine serum albumin (Sigma Aldrich, A7030-10G) dissolved in PBS for two hours, then washing three times for ten minutes with PBS with 0.05% Tween. Sections were incubated with biotinylated anti-rat, mouse and chicken Pax6 antibody (R&D Systems

Inc., #BAM1260) at a final concentration of 20 $\mu\text{g}/\text{mL}$ for two hours at room temperature and with Cy5-conjugated streptavidin (Invitrogen, #43-8316, diluted 1:50) for two hours at room temperature. Two fifteen-minute washes were implemented between each incubation period using PBS. Negative controls for antibody labeling underwent identical processing except that no primary antibody was added. Coverslips were mounted in 90% glycerol, and slides were stored at 4 °C until imaged. Images were obtained using an Olympus FV-1000 scanning confocal microscope. Confocal settings were initially optimized on an *E. sosorum* sample, and settings remained constant while acquiring each successive image. Negative controls for Pax6 staining can be found in [File S2](#).

Immunohistochemistry used to detect visual pigments in transverse sections of adult *E. rathbuni*, *E. nana*, and *E. sosorum* eyes followed the same protocol as above. Negative controls can be found in [File S3](#) for opsin and [File S4](#) for rhodopsin.

RESULTS

Adult ocular histology and measurements from early stage and adult eyes

Examination of adult ocular sections taken from two surface species and a subterranean species revealed markedly different histology between the two ecotypes. Histological sections from the surface species *Eurycea nana* and *E. sosorum* revealed well-defined retinal layers, corneal layers, iris, and lens ([Fig. 1](#)). A closer examination of the retinas ([Fig. 2](#)) consistently revealed seven layers we identified as retinal ganglion cell layer (RGL), inner plexiform layer (IPL), inner nuclear layer (INL), outer plexiform layer (OPL), outer nuclear layer (ONL), photoreceptors (PR), and retinal pigment epithelium (RPE). Although a nerve fiber layer was only sometimes apparent ([Fig. 1D](#)), a well-defined optic nerve was observed in both species. In the surface salamanders, melanized tissue was found primarily in the RPE, the choroid, and the ciliary body of the iris; however, some dark pigmentation was also observed outside the sclera and surrounding the optic nerve ([Fig. 2](#)). We additionally observed opsin and rhodopsin labeling in the two surface species (*E. sosorum* and *E. nana*); this labeling was absent in the subterranean species *E. rathbuni* ([Fig. 3](#)). Labeling in the two surface species was localized to the photoreceptor layer of *E. sosorum* and *E. nana* ([Fig. 3](#); white arrows).

Features previously described by [Eigenmann \(1900\)](#) for *Eurycea rathbuni* were identified and included (using his terminology) optic nerve (ON), three retinal layers, namely ganglion layer (GL), outer and inner reticular layer (O/IRL) and the pigment epithelium (PE). (Eigenmann may have used the term pigment epithelium (PE) because the pigmented layer in the eye of *E. rathbuni* appears to encompass the entire vestigial retina and is not restricted to its ancestral position sclerad to the photoreceptors as is the case for RPE.) No lens was identified in any adult *E. rathbuni*. A well-defined optic nerve was observed emanating from the eyes of *E. rathbuni* ([Fig. 4](#)). The entire ocular structure was surrounded by melanized tissue.

There were no significant differences ($P > 0.05$) in the overall thickness of the retina or the thickness of component layers when comparisons were made between sections taken

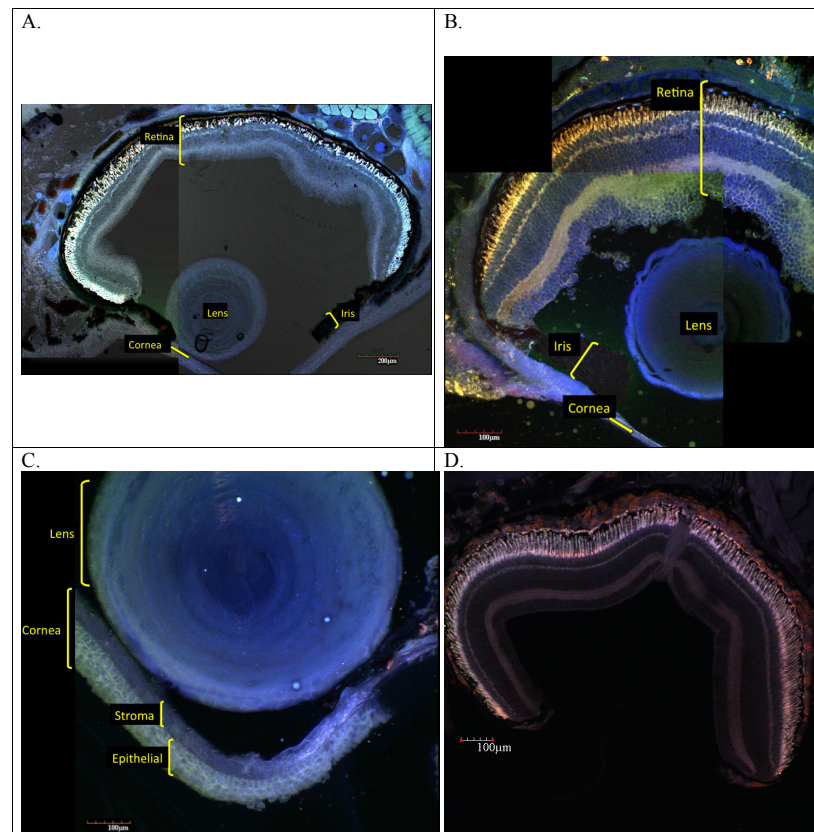


Figure 1 Sections of adult *E. nana* (A, C and D) and *E. sosorum* (B) eye. Using a laser scanning confocal microscope to detect autofluorescence from the sections, montages of images were produced using digitally applied pseudocolors to provide contrast. These images illustrate regions of the posterior eye showing well-developed retinal layers and pigment (A, B, D). The lens, cornea, and iris are also visible (A, B, C).

Full-size [DOI: 10.7717/peerj.11840/fig-1](https://doi.org/10.7717/peerj.11840/fig-1)

from *E. sosorum* and *E. nana* (File S5). The thickest layer of the retina in both species is the inner nuclear layer (INL), which contains the cellular nuclei of bipolar cells, horizontal cells and amacrine cells, and represents 22.9% of the retinal thickness in *E. nana* and 26.0% in *E. sosorum* (File S5).

We tested differences in eye size between *E. rathbuni* relative to *E. sosorum*. Measurements of the whole eye scaled to head length were obtained from animals early in development (stages 37 and 40) for *Eurycea rathbuni* ($n = 3$) and *E. sosorum* ($n = 3$) and from adult *E. rathbuni* ($n = 34$) and *E. sosorum* ($n = 34$) (Fig. 5). *E. nana* individuals were not included in this analysis as we did not have early developmental stages for this species. A one-way ANOVA and a post-hoc Tukey's HSD test revealed a difference between adult *E. sosorum* and all other groups (Tukey's HSD $P < 0.001$). There were no differences in the relative size of the eye between adult *E. rathbuni* and either species in their early developmental stages (Table 1).

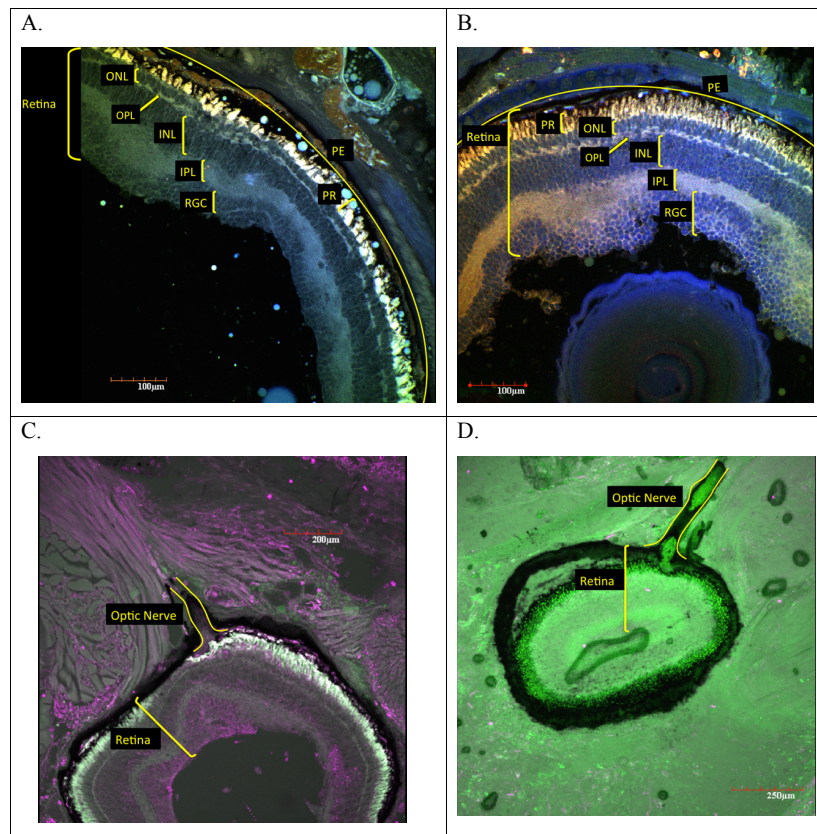


Figure 2 Ocular sections of adult *E. nana* (A, C) and *E. sosorum* (B, D). Using a laser scanning confocal microscope to detect autofluorescence from the sections, montages of images were produced using digitally applied pseudocolors to provide contrast. Ocular sections from adult *E. nana* (A and C) and adult *E. sosorum* (B and D) and associated retinal layers and optic nerve (C and D). Layers include pigment epithelium (PE), photoreceptor layer (PR), outer nuclear layer (ONL), outer plexiform layer (OPL), inner nuclear layer (INL), inner plexiform layer (IPL), and retinal ganglion cell layer (RGCL).

Full-size [DOI: 10.7717/peerj.11840/fig-2](https://doi.org/10.7717/peerj.11840/fig-2)

Developmental series and Pax6 localization

Staging was accomplished by following morphology for *E. sosorum* (Fig. 6) and *E. rathbuni* (Fig. 7). We were able to identify the following stages: stage 21 (embryos were defined as having neural folds closed to form neural tube), stages 25–26 (defined as having a prominent head, ear spot dorsal to the hyomandibular groove, and 9–10 somites), stage 31 (distinct gill folds), stage 37–38 (prominent gill folds, forelimb buds, and pigment migration from neural tube), and stage 40 (a prominent forelimb and hind limb bud, elongated and laterally compressed tail, pigmentation, and prominent eye spot) (Duellman & Trueb, 1986). The migration of melanocytes and concentrated pigmentation of the eye suggest ocular development (Figs. 6G, and 7G, black arrows).

Pax6 protein is observed in the two phenotypes represented by *E. rathbuni* (subterranean phenotype) and *E. sosorum* (surface phenotype). Labeling of Pax6 is also observed in and around the midbrain, optic cup, and lens vesicle of both species. The labeling of Pax6 in stage 40 of *E. rathbuni* is noticeably reduced compared to stage 37 in the same species

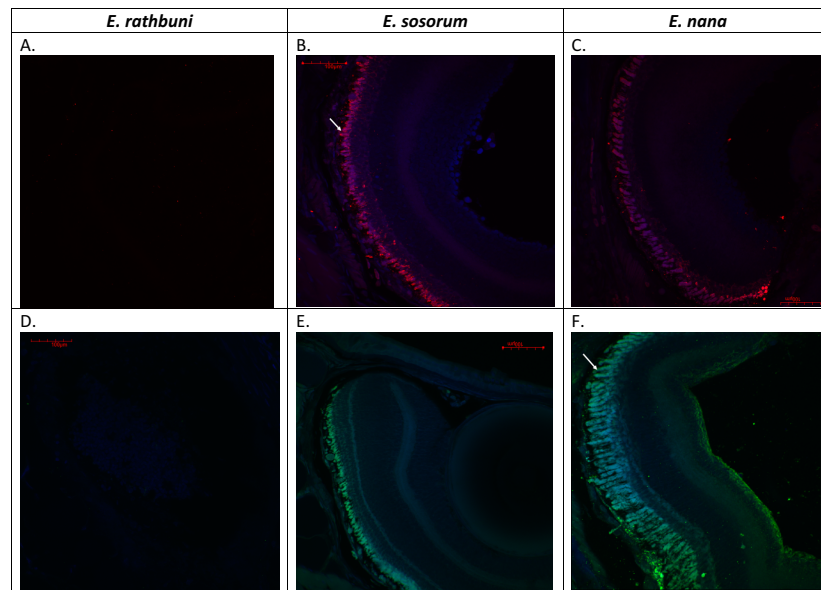


Figure 3 Adult *E. rathbuni*, *E. sosorum*, and *E. nana* retinal sections showing opsin and rhodopsin labeling. Images were acquired using a 20X water-immersion objective. Both surface species, *E. sosorum* (B & E) and *E. nana* (C & F) show labeling of opsin (A–C) and rhodopsin (D–F) in the photoreceptor layer of the retina (white arrows). No labeling is observed in the subterranean species *E. rathbuni* (A&D).

Full-size  DOI: 10.7717/peerj.11840/fig-3

and to both developmental stages of *E. sosorum*. Pax6 is strongly expressed in the tissue surrounding the developing optic cup of *E. sosorum*, and labeling is particularly noticeable within the lens of *E. sosorum* at stage 40 (Fig. 8).

DISCUSSION

This study provides a foundation of descriptive ocular histology comparing three closely related species and two ecotypes, surface and subterranean. *Eurycea rathbuni* has drastically reduced eyes, a characteristic widely accepted as reflecting adaptation to subterranean life and exemplified by other stygobitic organisms, including other cave-dwelling salamanders (e.g., *Proteus anguinus*), cave-dwelling fish (e.g., *Astyanax mexicanus*), as well as extremely phylogenetically divergent invertebrates (Romero, 2009). *E. rathbuni* exhibits a few vestigial retinal layers surrounded by melanized tissue. Were light available to this stygobitic salamander, it likely would be unable to pass through the pigmented cells surrounding the eye to be detected by photoreceptors. Nevertheless, the optic nerve is still present in *E. rathbuni* (Fig. 3), suggesting a possible sensory function, but probably not vision.

Upon close examination of *E. rathbuni* histology, the feature identified by Eigenmann (1900) as an optic nerve penetrating to the center of the eye resembles the hyaloid canal. The hyaloid canal provides vascularization to the developing lens during early embryogenesis (Dunlop, Moore & Beazley, 1997). Early hyaloid vascularization occurs when the hyaloid artery and vein follow the optic fissure via the optic stalk distally, eventually reaching the optic cup and lens vesicle, where they provide the necessary vascularization for the

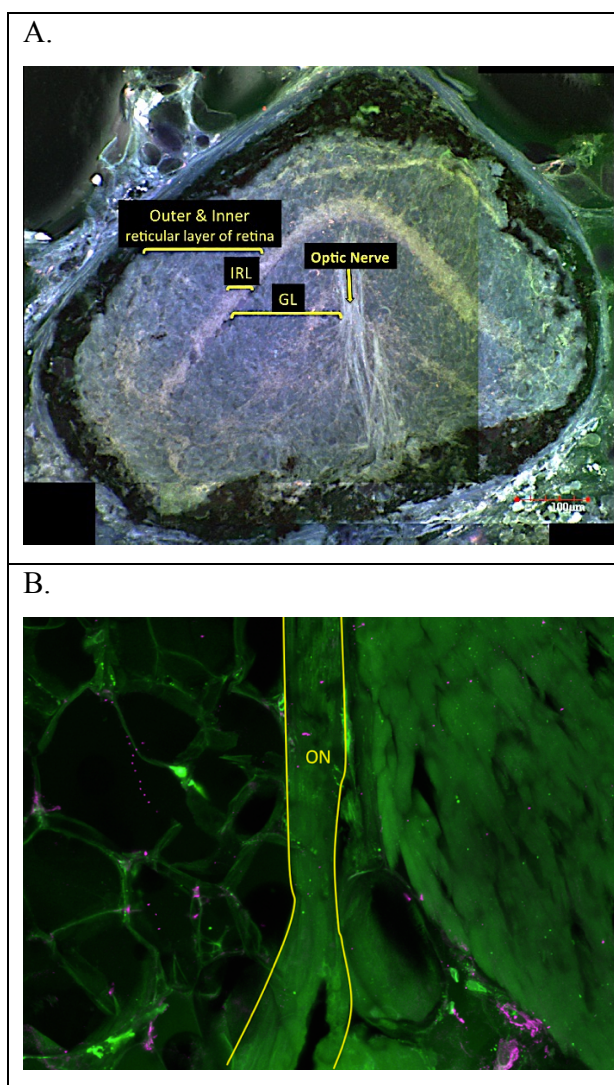


Figure 4 Adult *E. rathbuni* ocular sections. Sections showing undifferentiated tissue layers surrounded by pigment epithelium (A). The optic nerve is attached to the posterior region of the vestigial eye (A) and can also be seen at higher magnification and outlined in yellow (B). Sections are labeled after [Eigenmann \(1900\)](#) as follows: optic nerve (ON), ganglion layer (GL), inner reticular layer (IRL), outer and inner reticular layer of the retina.

Full-size DOI: [10.7717/peerj.11840/fig-4](https://doi.org/10.7717/peerj.11840/fig-4)

continued development of the lens. We found that ocular development in *E. rathbuni* progresses to the point of an optic cup and lens vesicle (Fig. 8). Therefore, it is likely that hyaloid vascularization is present during development. Nevertheless, a structure resembling the optic nerve clearly exits the eye, raising the question of what its function could be, given the light-free environment these animals occupy in nature and the melanized tissue completely surrounding the reduced eye. The optic nerve could be a vestige of the developmental pathway and processes that also facilitate forebrain development.

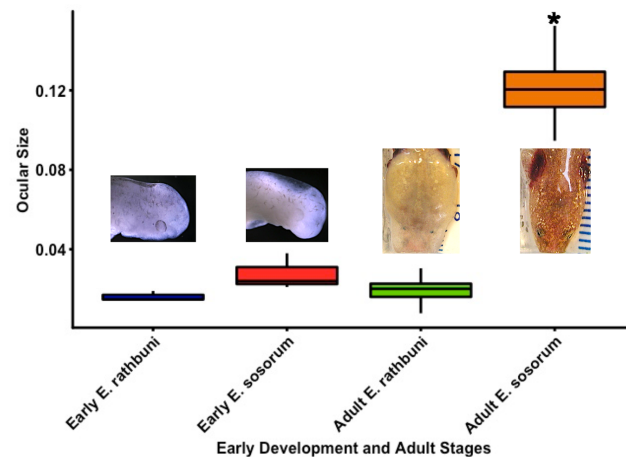


Figure 5 Normalized eye sizes for two species of salamander at different stages of development. Two developmental stages (early vs. adult) were measured and scaled to head size for two species from the central Texas *Eurycea* clade exemplifying subterranean (*E. rathbuni*) and surface (*E. sosorum*) optics. ANOVA and a post-hoc Tukey's test revealed that the ocular size of the adult *E. sosorum* was statistically significantly larger than the early stage *E. sosorum* and early and adult *E. rathbuni*. In contrast, there was no statistically significant difference between the ocular length of adult *E. rathbuni* and either embryonic salamander.

Full-size DOI: 10.7717/peerj.11840/fig-5

Table 1 One way ANOVA comparing eye size including early development and adult stages of *E. rathbuni* and *E. sosorum*.

	Early <i>E. rathbuni</i>	Early <i>E. sosorum</i>	Adult <i>E. rathbuni</i>
Early <i>E. sosorum</i>	$P > 0.05$	–	–
Adult <i>E. rathbuni</i>	$P > 0.05$	$P > 0.05$	–
Adult <i>E. sosorum</i>	** $P < 0.001$	** $P < 0.001$	** $P < 0.001$

We propose further investigations to track development and characterize these structures. When focusing on other regions of the eye like the retina, we could not distinguish retinal layers in the last stage of the subterranean species' developing eye; however, we do observe an optic cup in both stages.

The black *Proteus anguinus parkelj* develops a lens and a photoreceptor layer of the retina. The blind *P. anguinus anguinus* develops a cluster of lens precursor cells and has partially developed photoreceptor disks (Kos, Bulog & Röhlich, 2001). A close relative to the Texas *Eurycea* clade, the Georgia blind salamander (*Eurycea wallacei*) retains a rudimentary lens in at least half of the individuals sampled by Brandon (1968). A number of stygobitic teleost systems have been explored, including *A. mexicanus* (Jeffery, 2009), *P. andrussii* (Stemmer et al., 2015), and *Sinocyclocheilus anophthalmus* (Meng et al., 2013). Some terrestrial species like mammals (e.g., the genus *Spalax*), caecilians, and snakes show a range of underdevelopment in their eyes; the underdevelopment is thought to be associated with the dim-light environment of fossorial living (Carmona, Jiménez & Collinson, 2008; Simões et al., 2015). For the most part these species retain a lens, retinal layers, and some

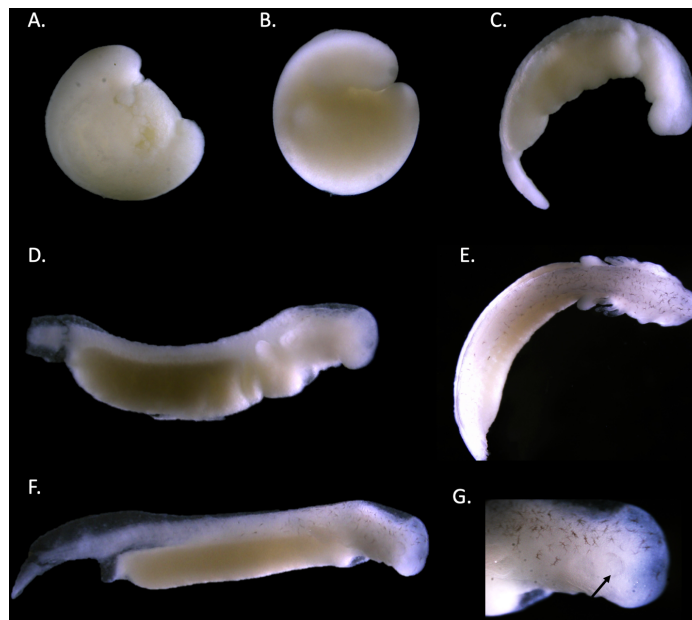


Figure 6 Staging of the Barton Springs salamander (*E. sosorum*). Stages are assigned based on morphology (Duellman & Trueb, 1986). Stages are as follows: Stage 21 (A). Stage 25–26 (B). Stage 31 (C). Stage 34 (D). Stage 37–38 (E). Stage 40 (F & G). Pigment accumulation (black arrow) around the developing eye in stage 40 is noted (G).

Full-size  DOI: 10.7717/peerj.11840/fig-6

amount of photoreceptor development. These observations illustrate that early ocular development of the vertebrate eye is mostly conserved.

Phylogenetic studies suggest the ancestor of *Eurycea rathbuni* had well-developed eyes, similar to extant epigeic species from this genus (e.g., *E. sosorum*) (Chippindale *et al.*, 2000; Wiens, Chippindale & Hillis, 2003; Sweet, 1984). The surface species *E. nana* and *E. sosorum* have well developed retinal layers, including photoreceptors and retinal pigment epithelium, exhibiting ocular anatomy expected of species endowed with vision (Linke, Roth & Rottluff, 1876; Heatwole, 1998). These surface species exhibit a lens, cornea, iris, and a well-developed optic nerve. Taken together, it appears that all the ocular structures necessary to support vision are in place.

When eye size was compared among early developmental stages and adults of *E. rathbuni* and *E. sosorum*, no differences were observed between adult *E. rathbuni* and either species' embryos (Fig. 4). This result suggests that the reduced eye size in *E. rathbuni* may reflect underdevelopment, i.e., a failure of development to progress. Fundamental knowledge of ocular anatomy has important implications for current research involving the central Texas *Eurycea*. For example, the full extent of visual function in the surface species may affect mate choice and predator or prey recognition (Fite, 1976; Roth, 1987). Future quantification of photoreceptors and their associated wavelength optima could elucidate the extent of color perception (Himstedt, Helas & Sommer, 1981; Korenyak & Govardovskii, 2013; Mohun & Davies Wayne, 2019) and the preferred active time during the day (e.g., nocturnal, diurnal, or crepuscular). Opsin and rhodopsin labeling in adult eye sections of

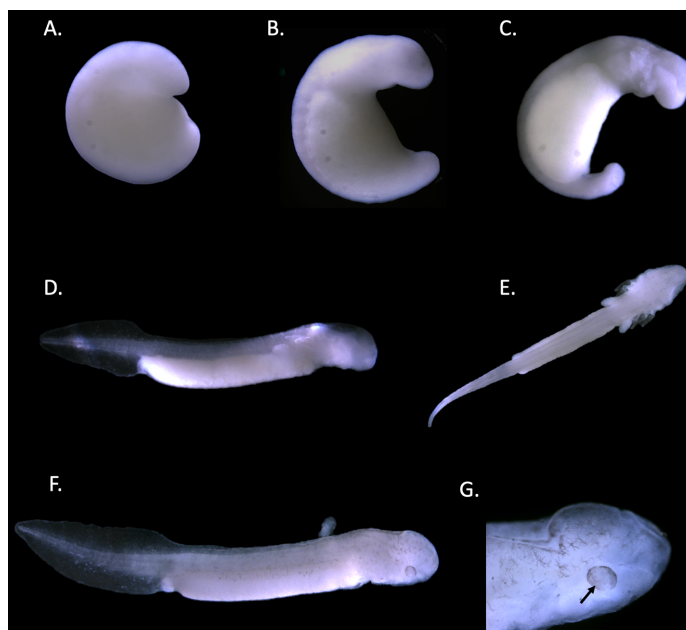


Figure 7 Staging of the Texas blind salamander (*E. rathbuni*). Stages are assigned based on morphology (Duellman & Trueb, 1986). Stages are as follows: Stage 21 (A). Stage 25–26 (B). Stage 31 (C). Stage 34 (D). Stage 37–38 (E). Stage 40 (F & G). Pigment accumulation (black arrow) around the developing eye in stage 40 is noted (G).

Full-size  DOI: [10.7717/peerj.11840/fig-7](https://doi.org/10.7717/peerj.11840/fig-7)

all *E. nana* and *E. sosorum* was associated with the outer segment of the photoreceptors. The morphology of the outer segments suggested rods dominate the photoreceptor layer in both surface species. Rods function during scotopic, or low light, vision, while cones are mostly responsible for photopic (bright light and color) vision. The retention of rods and their photo-responsive pigment (rhodopsin) in amphibians adapted to dark habitats (e.g., caecilians and *Proteus anguinus*) may provide some maintenance of photoperiodic perception (Mohun & Davies Wayne, 2019; Kos, Bulog & Röhlich, 2001). However, we observe neither morphologically distinct photoreceptors nor visual pigment labeling in the subterranean *E. rathbuni*.

One objective of this study at the outset was to examine expression of the homeobox gene *pax6* during the development of the eye in surface and subterranean salamanders. Pax6 is well known to drive eye development in a range of widely divergent animals, including both vertebrates and invertebrates (Kumar & Moses, 2001). Unfortunately, we only had 1–2 sections for each species at each stage that were suitable for labeling and comparison—too few to quantify labeling. However, given the rarity of such specimens and the similarity in pattern to what has been observed in *Asytanax*, we offer a preliminary, descriptive comparison of Pax6 localization between *E. rathbuni* and *E. sosorum*.

Compared spatially, the localization of Pax6 proteins through development of *E. rathbuni* and *E. sosorum* is similar and follows what is expected during vertebrate neurulation. Specifically, *pax6* is expressed in the developing central nervous system, including the

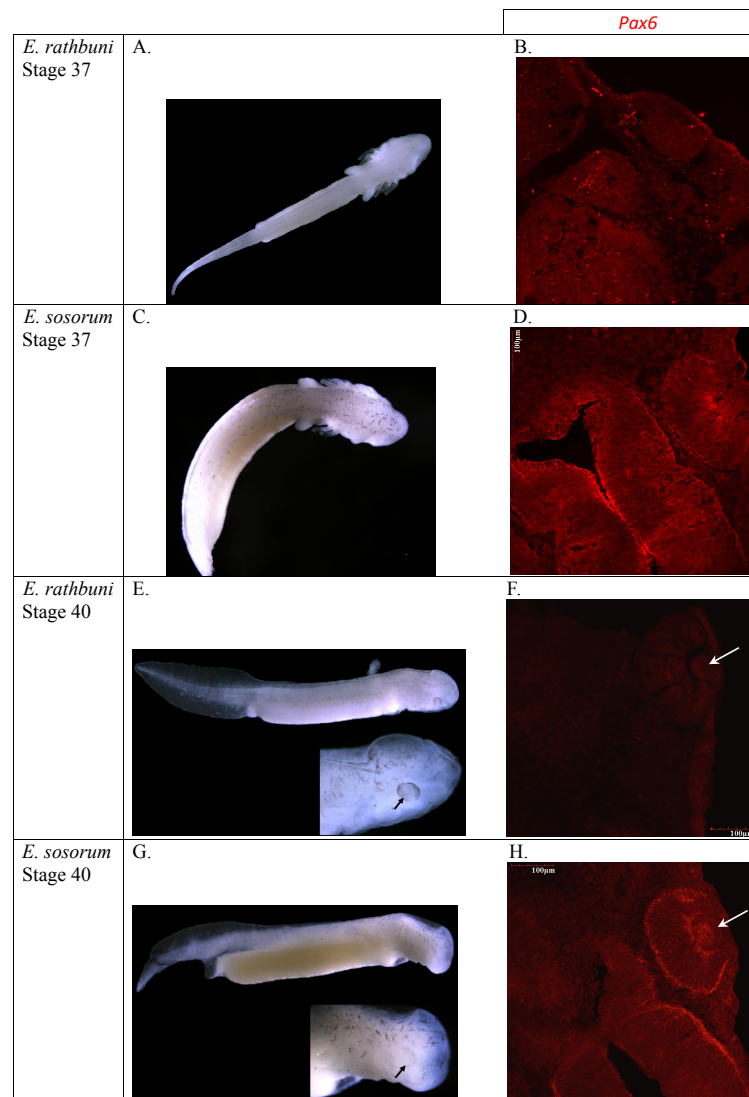


Figure 8 *E. rathbuni* and *E. sosorum* embryos at two stages of development and sections illustrating Pax6 labeling. The top two rows (A–D) of images show embryos at stage 37 (A & C) with their respective histological sections (B & D); the bottom two rows (E–H) of images show embryos at stage 40 (E & G) with black arrows indicating eye development. Histological sections for stage 40 (F & H) show labeling for Pax6 and lens development (white arrows). The image of a histological section through the anterior part of a stage 37 *E. rathbuni* embryo shows tissue positive for Pax6 labeling, where aggregates (not labeling; B) of secondary antibody are also evident (negative controls: [File S2](#)).

Full-size  DOI: [10.7717/peerj.11840/fig-8](https://doi.org/10.7717/peerj.11840/fig-8)

brain and eye ([Wawersik & Maas, 2000](#)). The continued expression of *pax6* and *vax1* genes is important as they encode transcription factors that bind with the enhancer sequence of the α -crystallin gene, which in turn encodes δ -crystallin proteins found in the lens ([Wawersik & Maas, 2000](#)). With noteworthy exceptions, if *pax6* expression is down regulated during the development of the lens, the lens will cease to develop ([Carmona et al., 2010](#)). In the subterranean fish *Asytanax mexicanus*, the down regulation of *pax6* gene consequent to

upregulation of *shh* expression contributes to apoptosis of the lens, which stunts further retinal differentiation and results in the formation of vestigial remnants of retina (Jeffery, 2005).

The ocular histology of adult *Eurycea sosorum* reveals a well-organized retina, suggesting a functional eye and by extension canonical expression of morphogens associated with eye development. In the newt *Cynops pyrrhogaster*, *pax6* gene expression persists through adulthood and plays an important role in regeneration when the animal is subjected to retinal injury (Del Rio-Tsonis, CH & Tsonis, 1995). In *E. rathbuni* the presence of Pax6 protein is noted early in development at stage 37 and is spatially distributed in the developing brain and eye in a pattern similar to that seen in *E. sosorum*. However, Pax6 was not detected at stage 40, suggesting diminished expression in *E. rathbuni*. Otherwise, patterns of ocular development observed in *E. sosorum* also occur in *E. rathbuni*, particularly in the development of a lens in the subterranean *E. rathbuni*. Therefore, it appears that some degree of lens development may occur in all vertebrate systems that live in dim to no light environments, and also exhibit reduced optics. Lens development in dim to no light systems occurs in fossorial mammals, e.g., *Talpa occidentalis* (Carmona, Jiménez & Collinson, 2008); the cave and aquifer teleosts *Astyanax mexicanus* (Jeffery, 2009), *Phreatichthys andruzzii* (Stemmer et al., 2015), and *Sinocyclocheilus anophthalmus* (Meng et al., 2013); and cave and deep aquifer Caudates, *Proteus anguinus* (Durand, 1976), *E. wallacei* (Brandon, 1968), and now *E. rathbuni* as demonstrated here. This observation also brings to light the far-reaching constraint and convergence in the process leading to an underdeveloped eye. Together, both the development of a lens and the localization patterns of Pax6 observed in *E. rathbuni* suggest parallel ocular development with *A. mexicanus*.

Low levels of Pax6 may explain the underdevelopment of the eye of *Eurycea rathbuni*. Investigation of Pax6 and Shh protein levels in later stages of *E. sosorum* and *E. rathbuni* is needed to understand the completion of retinal development in *E. sosorum* and lens degeneration in *E. rathbuni*. Moreover, examining later stages would illuminate the molecular underpinnings of lens degeneration and enable one to specifically address the role of apoptosis as a means to eye regression as seen in *Astyanax mexicanus*. Importantly, the overall ontogeny and localization of the Pax6 protein during ocular development of the two salamander phenotypes parallel the two phenotypes explored in *A. mexicanus* (Jeffery, 2009). This parallel suggests that the salamanders examined in this study and the teleost fish examined by Jeffery (2009) may share a degree of convergent evolution in development and in the molecular mechanisms (*pax6*) responsible for the divergent ocular phenotypes in two vertebrate lineages, fish and salamander, occupying similar subterranean habitats. Studies incorporating intermediate stages are needed to determine the divergence of tissue and gene expression between the epigeal and subterranean phenotypes, and if, as reported by Jeffery (2009), these early expression patterns lead to apoptosis of the lens.

CONCLUSIONS

The comparative examination of ocular histology suggests *Eurycea nana* and *E. sosorum* are capable of vision while development of the retina in *E. rathbuni* is aborted prior

to hatching, and the lens is lost at some point during ontogeny. We observed similar early ocular development between the two phenotypes, including the development of a lens in *E. rathbuni*. Taken together, parallels during early embryonic development were observed between the two phenotypes, whilst ocular morphology and histology in adults is drastically different. These results raise interesting questions about the evolution of subterranean phenotypes and the selective pressures they experience, how eyes are lost and what the molecular mechanisms responsible for ocular development and loss of eyes are.

As a vertebrate eye develops multiple genes are transiently expressed. Some of the most conserved are observed during early development (e.g., *pax6* and *shh*), and as tissues continue to differentiate, genes specific to those tissues are expressed (e.g., *cry* and *opsin*; (Zuber *et al.*, 2003). In the evolution of a reduced eye, these gene networks are also thought to reflect molecular evolutionary processes. Studies have identified different networks associated with species exhibiting reduced eyes (Emerling & Springer, 2014; Simões *et al.*, 2015; Protas *et al.*, 2006). We are working to identify the molecular networks involved in eye development in the central Texas *Eurycea*.

This study provides a platform using a stygobitic tetrapod to understand the evolutionary developmental biology of eye reduction. Moreover, a non-transgenic tetrapod model may provide novel insight to the genes and their regulation in developing a healthy eye. In the future, we hope to use multiple species from this clade and sequencing approaches incorporating intermediate stages to better understand the evolution and underlying genetic mechanisms responsible for the diverse subterranean phenotypes.

ACKNOWLEDGEMENTS

We thank the US Fish and Wildlife Service San Marcos Aquatic Recourse Center for continued support of this research, including access to facilities and captive populations of salamanders. We thank Drs. Nihal and Sunethra Dharmasiri for generously allowing the authors to image using their stereomicroscope. We also thank the reviewers of PeerJ for insightful comments.

ADDITIONAL INFORMATION AND DECLARATIONS

Funding

This work was supported by the East Texas Herpetological Society, South Texas Herpetological Society, Southwestern Association of Naturalist Howard McCarley Student Research Award, Herpetologists' League Jones-Lovich in Southwestern Herpetology Award, and Texas State University Thesis Research Support Fellowship. The confocal microscope was purchased with funds from NSF MRI grant DBI-0821252 awarded to Drs. Joseph R. Koke and Dana M. García at Texas State University. The funders had no role in study design, data collection and analysis, decision to publish, or preparation of the manuscript.

Grant Disclosures

The following grant information was disclosed by the authors:

The East Texas Herpetological Society.
South Texas Herpetological Society.
Southwestern Association of Naturalist Howard McCarley Student Research Award.
Herpetologists' League Jones-Lovich in Southwestern Herpetology Award.
Texas State University Thesis Research Support Fellowship.
NSF MRI: DBI-0821252.

Competing Interests

The authors declare there are no competing interests.

Author Contributions

- Ruben U. Tovar conceived and designed the experiments, performed the experiments, analyzed the data, prepared figures and/or tables, authored or reviewed drafts of the paper, and approved the final draft.
- Valentin Cantu, Brian Fremaux, Pedro Gonzalez Jr and Amanda Spikes analyzed the data, prepared figures and/or tables, authored or reviewed drafts of the paper, and approved the final draft.
- Dana M. García conceived and designed the experiments, prepared figures and/or tables, authored or reviewed drafts of the paper, and approved the final draft.

Animal Ethics

The following information was supplied relating to ethical approvals (i.e., approving body and any reference numbers):

Texas State University Institutional Animal Care and Use Committee (IACUC protocol approval number 0222_0530_12).

Data Availability

The following information was supplied regarding data availability:

The raw eye to head ratio measurements, control data Pax 6 images, control data for opsin images, control data for rhodopsin images and retinal thickness are available in the [Supplemental Files](#).

Supplemental Information

Supplemental information for this article can be found online at <http://dx.doi.org/10.7717/peerj.11840#supplemental-information>.

REFERENCES

- Bendik NF, Meik JM, Gluesenkamp AG, Roelke CE, Chippindale PT. 2013.** Biogeography, phylogeny, and morphological evolution of central Texas cave and spring salamanders. *BMC Evolutionary Biology* 13:201 DOI 10.1186/1471-2148-13-201.
- Brandon RA. 1968.** Structure of the eye of *Haideotriton wallacei*, a North American troglobitic salamander. *Journal of Morphology* 124(3):345–352 DOI 10.1002/jmor.1051240307.

- Carmona FD, Jiménez R, Collinson JM. 2008.** The molecular basis of defective lens development in the Iberian mole. *BMC Biology* **6**:44 DOI [10.1186/1741-7007-6-44](https://doi.org/10.1186/1741-7007-6-44).
- Carmona FD, Ou J, Jiménez R, Collinson JM. 2010.** Development of the cornea of true moles (Talpidae): morphogenesis and expression of PAX6 and cytokeratins. *Journal of Anatomy* **217**(5):488–500 DOI [10.1111/j.1469-7580.2010.01299.x](https://doi.org/10.1111/j.1469-7580.2010.01299.x).
- Chippindale P, Price A, Wiens J, Hillis D. 2000.** Phylogenetic relationships and systematic revision of central Texas hemidactyliine plethodontid salamanders. *Herpetological Monographs* **14**:1–80 DOI [10.2307/1467045](https://doi.org/10.2307/1467045).
- Chow RL, Altmann CR, Lang RA, Hemmati-Brivanlou A. 1999.** Pax6 induces ectopic eyes in a vertebrate. *Development* **126**(19):4213–4222 DOI [10.1242/dev.126.19.4213](https://doi.org/10.1242/dev.126.19.4213).
- Del Rio-Tsonis K, Washabaugh CH, Tsonis PA. 1995.** Expression of pax-6 during urodele eye development and lens regeneration. *Proceedings of the National Academy of Sciences of the United States of America* **92**(11):5092–5096 DOI [10.1073/pnas.92.11.5092](https://doi.org/10.1073/pnas.92.11.5092).
- Devitt TJ, Wright AM, Cannatella DC, Hillis DM. 2019.** Species delimitation in endangered groundwater salamanders: implications for aquifer management and biodiversity conservation. *Proceedings of the National Academy of Sciences of the United States of America* **116**:2624–2633 DOI [10.1073/pnas.1815014116](https://doi.org/10.1073/pnas.1815014116).
- Duellman WE, Trueb L. 1986.** *Biology of Amphibians*. Baltimore: The Johns Hopkins University Press, 109–132.
- Dunlop SA, Moore SR, Beazley LD. 1997.** Changing patterns of vasculature in the developing amphibian retina. *The Journal of Experimental Biology* **200**:2479–2492 DOI [10.1242/jeb.200.18.2479](https://doi.org/10.1242/jeb.200.18.2479).
- Durand JP. 1976.** Ocular development and involution in the European Cave Salamander, *Proteus anguinus* Laurenti. *The Biological Bulletin* **151**:450–466 DOI [10.2307/1540499](https://doi.org/10.2307/1540499).
- Eigenmann CH. 1900.** The eyes of the blind vertebrates of North America. II. The eyes of Typhlomolge rathbuni Stejneger. *Transactions of the American Microscopical Society* **21**:49–56, 58–60 DOI [10.2307/3221027](https://doi.org/10.2307/3221027).
- Emerling CA, Springer MS. 2014.** Eyes underground: regression of visual protein networks in subterranean mammals. *Molecular Phylogenetics and Evolution* **78**:260–270 DOI [10.1016/j.ympev.2014.05.016](https://doi.org/10.1016/j.ympev.2014.05.016).
- Emerson ET. 1905.** General anatomy of *Typhlomolge rathbuni*. *Proceedings of the Boston Society of Natural History* **32**:43–75.
- Fite KV. 1976.** The amphibian visual system. In: *A multidisciplinary approach*. London New York: Academic Press, 225–305.
- Goricki S, Niemiller ML, Fenolio DB. 2012.** In: White WB, Culver DC, eds. *Salamanders, encyclopedia of caves*. Massachusetts: Academic Press, Elsevier, 665–676.
- Heatwole H. 1998.** *Amphibian biology volume 3, sensory perception*. Chipping Norton: Surrey Beatty and Sons, 797–807.
- Himstedt W, Helas A, Sommer TJ. 1981.** Projection of color coding retinal neurons in urodele amphibians. *Brain Behavior and Evolution* **18**:19–32 DOI [10.1159/000121773](https://doi.org/10.1159/000121773).

- Jeffery WR. 2005.** Adaptive evolution of eye degeneration in the Mexican blind cavefish. *Journal of Heredity* **96**(3):185–196 DOI [10.1093/jhered/esi028](https://doi.org/10.1093/jhered/esi028).
- Jeffery WR. 2009.** Chapter 8. Evolution and development in the cavefish *Astyanax*. *Current topics in developmental biology* **86**:191–221 DOI [10.1016/S0070-2153\(09\)01008-4](https://doi.org/10.1016/S0070-2153(09)01008-4).
- Korenyak DA, Govardovskii VI. 2013.** Photoreceptors and visual pigments in three species of newts. *Journal of Evolutionary Biochemistry and Physiology* **49**:399–407 DOI [10.1134/S0022093013040038](https://doi.org/10.1134/S0022093013040038).
- Kos M, Bulog A, Szél B, Röhlich P. 2001.** Immunocytochemical demonstration of visual pigments in the degenerate retinal and pineal photoreceptors of the blind cave salamander (*Proteus anguinus*). *Cell and Tissue Research* **303**(1):15–25 DOI [10.1007/s004410000298](https://doi.org/10.1007/s004410000298).
- Krishnan J, Rohner N. 2017.** Cavefish and the basis for eye loss. *Philosophical Transactions of the Royal Society B: Biological Sciences* **372**:20150487 DOI [10.1098/rstb.2015.0487](https://doi.org/10.1098/rstb.2015.0487).
- Kumar JP, Moses K. 2001.** Expression of evolutionarily conserved eye specification genes during *Drosophila* embryogenesis. *Development Genes and Evolution* **211**(8–9):406–414 DOI [10.1007/s004270100177](https://doi.org/10.1007/s004270100177).
- Linke R, Roth G, Rottluff B. 1876.** Comparative studies on the eye morphology of lungless salamanders, family Plethodontidae, and the effect of miniaturization. *Journal of Morphology* **189**:131–143.
- Meng F, Braasch I, Phillips JB, Lin X, Titus T, Zhang C, Postlethwait JH. 2013.** Evolution of the eye transcriptome under constant darkness in *Sinocyclocheilus* cavefish. *Molecular Biology and Evolution* **30**(7):1527–1543 DOI [10.1093/molbev/mst079](https://doi.org/10.1093/molbev/mst079).
- Mitchell RW, Reddell JR. 1965.** *Eurycea tridentifera* a new species of troglobitic salamander from Texas and a reclassification of *Typhlomolge rathbuni*. *Texas Journal of Science* **17**:12–20.
- Mohun SM, Davies Wayne IL. 2019.** The evolution of amphibian photoreception. *Frontiers in Ecology and Evolution* **7**:321 DOI [10.3389/fevo.2019.00321](https://doi.org/10.3389/fevo.2019.00321).
- Möller A. 1951.** Die Struktur des Auges bei Urodelen verschiedener Körpergröße. *Zoologische Jahrbücher* **62**:138–182.
- Neve DL, Savage AA, Koke RJ, García DM. 2012.** Activating transcription factor 3 and reactive astrocytes following optic nerve injury in zebrafish. *Comparative Biochemistry and Physiology Part C: Toxicology & Pharmacology* **155**(2):213–218.
- Protas ME, Hersey C, Kochanek D, Zhou Y, Wilkens H, Jeffery WR, Zon LI, Borowsky R, Tabin CJ. 2006.** Genetic analysis of cavefish reveals molecular convergence in the evolution of albinism. *Nature Genetics* **38**(1):107–111 DOI [10.1038/ng1700](https://doi.org/10.1038/ng1700).
- Rétaux S, Casane D. 2013.** Evolution of eye development in the darkness of caves: adaptation, drift, or both? *EvoDevo* **4**:26 DOI [10.1186/2041-9139-4-26](https://doi.org/10.1186/2041-9139-4-26).
- Rohner DFJ, Kowalko JE, Yoshizawa M, Jeffery WR, Borowsky RL, Lindquist S, Tabin CJ. 2013.** Cryptic variation in morphological evolution: HSP90 as a capacitor for loss of eyes in cavefish. *Science* **342**:1372–1375.
- Romero A. 2009.** *Cave biology life in darkness*. New York: Cambridge University Press, 130–158.

- Roth G. 1987.** *Visual behavior in salamanders*. Germany: Springer-Verlag Berlin Heidelberg, 89–128.
- Saul KE, Koke JR, García DM. 2010.** Activating transcription factor 3 (ATF3) expression in the neural retina and optic nerve of zebrafish during optic nerve regeneration. *Comparative Biochemistry and Physiology, Part A* **155**:172–182 DOI [10.1016/j.cbpa.2009.10.042](https://doi.org/10.1016/j.cbpa.2009.10.042).
- Schneider CA, Rasband WS, Eliceiri KW. 2012.** NIH Image to ImageJ: 25 years of image analysis. *Nature Methods* **9**:671–675 DOI [10.1038/nmeth.2089](https://doi.org/10.1038/nmeth.2089).
- Simões BF, Sampaio FL, Jared C, Antoniazzi MM, Loew ER, Bowmaker JK, Rodriguez A, Hart NS, Hunt DM, Partridge JC, Gower DJ. 2015.** Visual system evolution and the nature of the ancestral snake. *Journal of Evolutionary Biology* **28**(7):1309–1320 DOI [10.1111/jeb.12663](https://doi.org/10.1111/jeb.12663).
- Stemmer M, Schuhmacher L-N, Foulkes NS, Bertolucci C, Wittbrodt J. 2015.** Cavefish eye loss in response to an early block in retinal differentiation progression. *Development* **142**(4):743–752.
- Sweet SS. 1984.** Secondary contact and hybridization in the Texas cave salamanders *Eurycea neotenes* and *E. tridentifera*. *Copeia* **2**:428–441.
- Walls G. 1942.** *The vertebrate eye and its adaptive radiation*. Bloomfield Hills: Cranbrook Institute of Science, Bull 19.
- Wawersik S, Maas RL. 2000.** Vertebrate eye development as modeled in *Drosophila*. *Human Molecular Genetics* **9**(6):917–925 DOI [10.1093/hmg/9.6.917](https://doi.org/10.1093/hmg/9.6.917).
- Wiens JJ, Chippindale PT, Hillis DM. 2003.** When are phylogenetic analyses misled by convergence? A case study in Texas cave salamanders. *Systematic Biology: A Journal of the Society of Systematic Biologists* **52**(4):501–514 DOI [10.1080/10635150309320](https://doi.org/10.1080/10635150309320).
- Zuber ME, Gestri G, Viczian AS, Barsacchi G, Harris WA. 2003.** Specification of the vertebrate eye by a network of eye field transcription factors. *Development* **130**(21):5155–5167 DOI [10.1242/dev.00723](https://doi.org/10.1242/dev.00723).